





Atmospheric Environment 42 (2008) 3751-3764



www.elsevier.com/locate/atmosenv

# Modeling the effects of ship emissions on coastal air quality: A case study of southern California

Satish Vutukuru, Donald Dabdub\*

Mechanical and Aerospace Engineering, University of California, 4226 Engineering Gateway, Irvine, CA 92617, USA

Received 11 July 2007; received in revised form 3 December 2007; accepted 25 December 2007

#### Abstract

Impact of emissions from ocean-going ships on ozone and particulate matter concentrations is quantified using UCI-CIT model for the South Coast Air Basin of California (SoCAB). The modeling domain encompasses Los Angeles and Long Beach ports and part of the Pacific Ocean that is traversed by ships to visit these ports. Impacts are assessed for a base year (2002) and a future year (2020) by analyzing results from simulations of a three-day summer episode. Contribution of ship emissions to peak 1-h and 8-h ozone concentrations is predicted to be up to 29 and 24 ppb, respectively, for the year 2002. Similarly, particulate nitrate and sulfate concentrations increase up to 12.8 and  $1.7 \,\mu g \, m^{-3}$ , respectively, in the basin when ship emissions are included. Maximum impacts are predicted to occur along the coasts of Ventura and Los Angeles and also at inland locations near Simi Valley. Future year simulations show substantial increase in impacts from ships due to expected growth in ship emissions. Ozone increases are as high as 59 ppb for land-based locations when estimates of ship emissions for 2020 are included. Similarly, particulate nitrate and sulfate increase up to 14 and  $2.5 \,\mu g \, m^{-3}$ . The results of this study show that control of ship emissions is important to mitigate air pollution. © 2008 Elsevier Ltd. All rights reserved.

Keywords: Urban air quality; Ship emissions; Ozone; Atmospheric aerosols; Regional modeling

#### 1. Introduction

Ship emissions are becoming a significant source of air pollution in cities near major ports. Recent estimates of global sulfur and nitrogen oxide emissions from international shipping are 6.49 Tg S and 6.87 Tg N, respectively (Corbett and Koehler, 2003). Emission containing oxides of nitrogen  $(NO_x)$  and sulfur  $(SO_x)$  are processed by atmospheric chemical and physical mechanisms resulting

\*Corresponding author. Tel.: +19498246126; fax: +19498248585.

E-mail address: ddabdub@uci.edu (D. Dabdub).

in the formation of secondary pollutants such as ozone and particulate matter (PM). Although ship emissions currently constitute only a small fraction of total global emissions, they could have important environmental effects on coastal areas near ports with heavy ship traffic as shown in studies for regions in Europe, Asia and North America (Dore et al., 2007; Derwent et al., 2005; Endresen et al., 2003; Lu et al., 2006; Streets et al., 2000).

According to the International Maritime Organization (2000), 80% of shipping traffic occurs in the Northern Hemisphere of which 75% occurs within 400 km from coast. Emissions from such shipping activities undergo atmospheric transport and may

affect coastal air quality. Environmental regulation over past two decades led to the reduction of emissions from land-based sources. However, today ships represent a major unregulated source category. Furthermore, emissions from shipping activities are growing. Ship emissions will increase significantly in next 10–40 years owing to expanding international commerce (Eyring et al., 2005). As a result, it is necessary to understand atmospheric impacts of these emissions, especially on regional air quality.

This study evaluates the impacts of ship emissions on ambient ozone and PM concentrations in the South Coast Air Basin of California (SoCAB) for the first time. The South Coast Air Basin contains Los Angeles and Long Beach ports. The Los Angeles port is the busiest port in United States, followed by the neighboring Long Beach port, in terms of cargo volume processed (BST Associates, 2007). The two port complexes combined form the fifth-largest port complex of the world, bringing in about one-third of total container cargo arriving to the United States. Ships that visit these ports are mostly ocean-going vessels carrying containerized cargo and liquid fuels.

Ocean-going vessels are propelled by two-stroke diesel engines with power ranging from 10 to 70 MW. These engines run on distillate or residual fuel, emitting high levels of  $NO_x$ ,  $SO_x$  and PM. Further, such marine fuels contain high levels of sulfur, resulting in particularly high levels of  $SO_x$  emissions. For instance, the world-wide average sulfur content in marine fuels is 2.7% (27,000 ppm) (Entec, 2002), while the state of California's sulfur limit for on-road diesel is 0.0015% (15 ppm). Therefore, contribution of ship emissions to ambient sulfates is of particular interest.

Previous studies evaluated the impact of ship emissions focusing on global issues. Lawrence and Crutzen (1999) showed increase in surface ozone and OH radical concentrations when  $NO_x$  emissions from ships are included in a global chemistry-transport model. Similarly, Capaldo et al. (1999) calculated an increase of  $SO_2$  concentrations as high as 60% when sulfur emissions from ships are included in to a global model. Ship emissions also lead to increase in aerosol production through enhancement of OH radical concentration. A 30% increase in sulfate aerosol is predicted due to sulfur emission from ships (Capaldo et al., 1999). Streets et al. (2000) concluded that parts of Southeast Asia receive significant amounts of sulfur deposition due

to ship emissions. More recently, studies with updated emission inventories show a maximum perturbation of 12 ppb for tropospheric ozone concentrations (Endresen et al., 2003). Derwent et al. (2005) applied a Lagrangian chemistry-transport model and showed that contribution of ships to sulfur deposition is as high as 55% for some locations in Europe. Although global and continental scale modeling studies established the importance of ship emissions, there are only few studies available that quantify the impact of ship emissions on smaller scales using high-resolution models. This study bridges that gap by conducting a modeling study for a region with two busy ports in an urban airshed.

# 2. Methodology

In Southern California, high levels of ozone occur during the summertime due to high temperatures and stagnant conditions. High ozone enhances the formation of secondary PM, also leading to high levels of PM (Meng et al., 1997). Therefore, a summer episode is selected for this study. Air quality impacts of ship emissions are quantified by analyzing the difference between model-predicted ambient concentrations that include ship emissions and those that do not include ship emissions. The 8-h and 1-h average concentrations are used to analyze ozone impacts and 24-h average concentrations are used for PM impacts.

Air quality simulations are performed using the UCI-CIT model. The UCI-CIT model was developed at the California Institute of Technology (Harley and Cass, 1994) and is now under continuous development at the University of California, Irvine. The model incorporates stateof-science modules to simulate the atmospheric chemistry, transport and aerosol formation processes to predict spatial and temporal distribution of atmospheric trace gases and particles. The UCI-CIT model has been applied extensively for atmospheric studies for the southern California region: investigation of chlorine chemistry (Knipping and Dabdub, 2003); study of the coupling between PM and NO<sub>x</sub> and VOC emission controls (Nguyen and Dabdub, 2002a); calculation of incremental aerosol reactivity (Carreras-Sospedra et al., 2005); assessment of air quality impacts from distributed power generation (Rodriguez et al., 2006); and dynamics of secondary organic aerosol (Vutukuru et al., 2006).

The UCI-CIT model solves numerically mass conservation equations for modeled species on a computational grid to obtain spatially and temporally resolved concentrations of gas and aerosol species of interest. Atmospheric gas-phase chemistry is modeled using the Caltech atmospheric chemical mechanism (CACM) (Griffin et al., 2002). The CACM mechanism is a lumped species mechanism that includes detailed chemistry of organic compounds in air quality simulations. CACM includes a total of 191 species, of which chemistry of 120 species is tracked explicitly, 67 species are assumed to be pseudo-steady-state and 4 species are constant.

Inorganic aerosol calculations are performed simulating atmospheric equilibrium (SCAPE2) (Meng et al., 1995, 1998). Aerosol concentrations are resolved into eight size bins and are obtained by solving the condensation/evaporation equation in a fully dynamic fashion (Meng et al., 1998). An operator-splitting technique (McRae and Seinfeld, 1982) is implemented to decouple the individual processes and obtain a numerical solution. This technique provides flexibility to use different numerical schemes for each numerical operator (i.e. atmospheric mechanism that affects concentration of modeled species). For this study, the Quintic Splines Taylor Series Expansion (QSTSE) algorithm is used to solve the advection equation (Nguyen and Dabdub, 2001). The condensation/evaporation equation associated with inorganic aerosol dynamics is solved by the partitioned flux integrated semi-Lagrangian method (PFISLM) (Nguyen and Dabdub, 2002b).

The UCI-CIT model has been evaluated in previous studies using data from extensive field campaigns. Meng et al. (1998) and Griffin et al. (2002) studied the model performance for predictions of aerosol and ozone concentrations, respec-

tively. In addition to model validation, extensive sensitivity studies are conducted for the model. Carreras-Sospedra et al. (2006) evaluated model sensitivity to input meteorological, boundary and initial conditions and model components. Rodriguez and Dabdub (2003) used Monte Carlo methods to study uncertainty and sensitivity of CACM mechanism to model inputs.

# 2.1. Model configuration

The modeling domain for this study is shown in Fig. 1 and covers the SoCAB of California. The modeling domain includes port complexes of Los Angeles and Long Beach, part of Pacific Ocean that contain shipping lanes traversed by ships visiting these ports along the coasts of Santa Barbara and Ventura. The model domain is divided in to a computational grid of  $80 \times 30$  cells in the horizontal dimension of  $5 \times 5 \, \mathrm{km}^2$  resolution. In the vertical dimension, the model domain is resolved in to 5 layers up to 1100 m using terrain following coordinates.

The UCI-CIT model requires gridded fields of hourly meteorological parameters (temperature, wind and relative humidity) and basin-wide emission inventories. Meteorological data are used from a field campaign conducted in 1987 that enables to simulate a three-day air quality episode. This data set was collected during the Southern California Air Quality Study (SCAQS), an extensive campaign of atmospheric measurements that occurred in the SoCAB during 27–29 August 1987. This data set was used to validate the UCI-CIT model in several air quality studies (Meng et al., 1998; Griffin et al., 2002). Furthermore, the South Coast Air Quality Management District of California used this data set to develop air pollution control strategies in

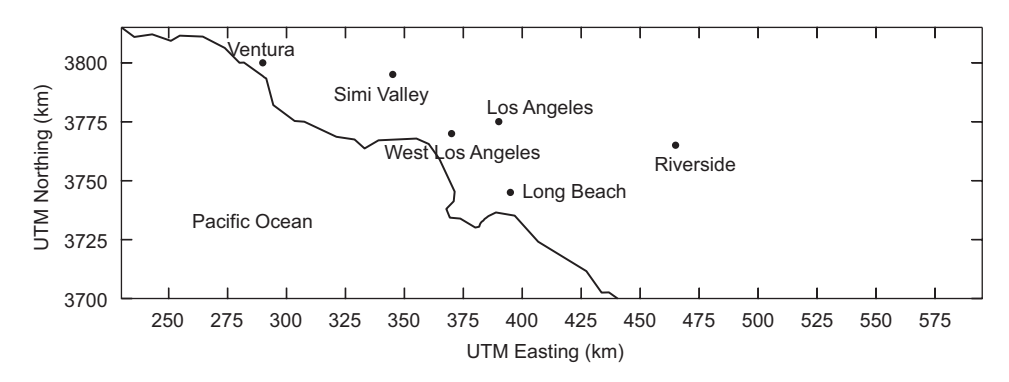


Fig. 1. Modeling domain of the study that covers most of the South Coast Air Basin of California.

order to attain ozone attainment by 2010. Zeldin et al. (1990) showed that this episode is statistically within top 10% of severe ozone-forming metrological conditions.

In the SoCAB, dominant direction of wind is from west (Pacific Ocean) to east (inland locations) resulting from onshore pressure gradients. The meteorological conditions during the SCAQS episode are representative of this pattern, resulting in emissions from urban areas around Los Angeles being transported to inland areas around Riverside in the eastern part of the domain. During the SCAOS episode, temperatures ranged from moderate  $(15-20 \,^{\circ}\text{C})$  in the night to high  $(40-42 \,^{\circ}\text{C})$  at inland locations in the afternoon. Further, a welldefined diurnal inversion layer formed at the top of neutral/unstable layers near the surface and a slightly stable boundary layer during the night led to low mixing heights ( $\sim$ 50–1100 m) during the episode. Low mixing heights lead to limited vertical mixing, and thus causing high concentration of pollutants due to accumulation. Carreras-Sospedra et al. (2006) provides further description on meteorological aspects of this episode.

# 2.2. Ship and land-based emissions in Southern California

Estimation of emissions from shipping activities is a challenging exercise, as such task requires extensive data on ship traffic, characteristics of ships such as engine size, fuel and power usage and finally estimates of emission factors. A global geographically-resolved emission inventory developed by Corbett and Fischbeck (1997) was used in early global modeling studies that showed the importance of ship emissions (Capaldo et al., 1999). In the following years, several estimates of ship emissions were developed using various assumptions and data sources (Corbett et al., 1999, 2003; Endresen et al., 2003; Richter et al., 2004).

This work uses the latest ships emission inventory recently developed by Corbett et al. (2007). The new inventory represents the most recent estimate currently available for ship emissions from oceangoing commercial and passenger vessels in the North American region (Wang et al., 2007). The inventory was developed using a bottom-up methodology to obtain a spatially resolved inventory using historical ship movements, ship attributes and ship emission factors. Aggregated estimates of monthly emissions for North American region are

available for years 2002, 2010 and 2020. August estimates are used in order to evaluate the impact of ship emissions during summer months.

Air quality models simulate episodes of few days using emissions data that are resolved in spatial and temporal dimensions and chemical speciation. The UCI-CIT model requires hourly and speciated emissions data over the modeling region. Two assumptions are made in order to develop emission inventories using aggregated data from Corbett et al. (2007). First, daily emissions for summertime are obtained from aggregated geographically resolved August month emissions by dividing by 31, i.e. assuming that total emissions do not differ significantly on daily basis for a given month. The hourly resolved emissions are obtained by assuming uniform distribution during the day. However, ship emissions are expected to show some diurnal and weekly variation as port operations occur mostly during the day on weekdays. Therefore, a parametric analysis is conducted to evaluate the effect of temporal profile of ship emissions. In the first scenario that accounts for diurnal variation, 70% of total daily ship emissions occur between 8 AM and 8 PM and 30% occur between 8 PM and 8 AM. In the second scenario, the first day of the three-day episode is assumed to be a weekend day or a holiday, followed by two weekday emissions. Ship emissions during the weekend day are assumed to be at 50% of weekday emissions, keeping the total emissions during the month as estimated by Corbett et al. (2007). Model results from air quality simulation of these scenarios show that although impacts of ship emissions depend on temporal profile, only small differences are observed in comparison with the case that assumes uniform emissions. Therefore, the assumption of uniform rate of emissions serves well in the absence of highresolution ship emissions data.

Second assumption relates to speciation of hydrocarbon and PM emission from ships as such data are currently not available. This study uses the California Air Resources Board (CARB) profile of internal combustion engine using distillate fuel that closely represents engines used to power oceangoing vessels. Similarly, speciation and size-distribution of PM emissions are obtained from CARB speciation profile for the combustion of distillate fuel. As per CARB size-distribution profile, 95% of particles are in PM<sub>2.5</sub> and 97% are in PM<sub>10</sub> size ranges. The composition of PM<sub>2.5</sub> and PM<sub>10</sub> is dominated by sulfates due to high content of sulfur

in the distillate fuel. As per CARB speciation profile, 44% of  $PM_{2.5}$  and 50% of  $PM_{10}$  direct emissions are assumed to be sulfate particles.

Land-based emissions include gridded fields of both surface and elevated emissions. These emissions are developed using the SoCAB emission inventory for the year 1997, which was used in the development of South Coast air quality management plan. The 1997 inventory is scaled to the level of year 2002 emissions using county-wide aggregate data available from CARB. The summary of

domain-wide emissions with and without ship emissions is shown in Table 1. Daily  $NO_x$  and  $SO_x$  emissions from ships in the modeling domain are 38.4 and 22.8 ton, respectively, for the year 2002. Ships contribute up to 25% of total  $SO_x$  emissions in the modeling domain. As mentioned before, this is due to the use of fuel with high sulfur content.  $NO_x$  emissions are at about 7% of total domain-wide emissions. VOC and PM emissions are less than 1%. Figs. 2(a)–(d) show geographic distribution of total  $NO_x$  and  $SO_x$  emissions in the domain

Table 1 Summary of daily domain-wide emissions for years 2002 and 2020

Without ship emissions (ton day		With ship emissions Emissions from ships $(\tan day^{-1})$ $(\tan day^{-1})$		Ship emissions as percentage o total basin-wide emissions (%)		
2002 case						
$NO_x$	874.5	912.9	38.4	4.2		
$SO_x$	72.0	94.8	22.8	24.1		
VOC	580.0	582.9	2.9	0.50		
PM	1215.5	1216.4	0.9	0.07		
2020 case						
$NO_x$	305.8	403.7	97.9	24.2		
$SO_x$	93.6	157.2	59.1	40.5		
VOC	662.4	671.2	8.8	1.3		
PM	741.9	744.9	3.0	0.40		

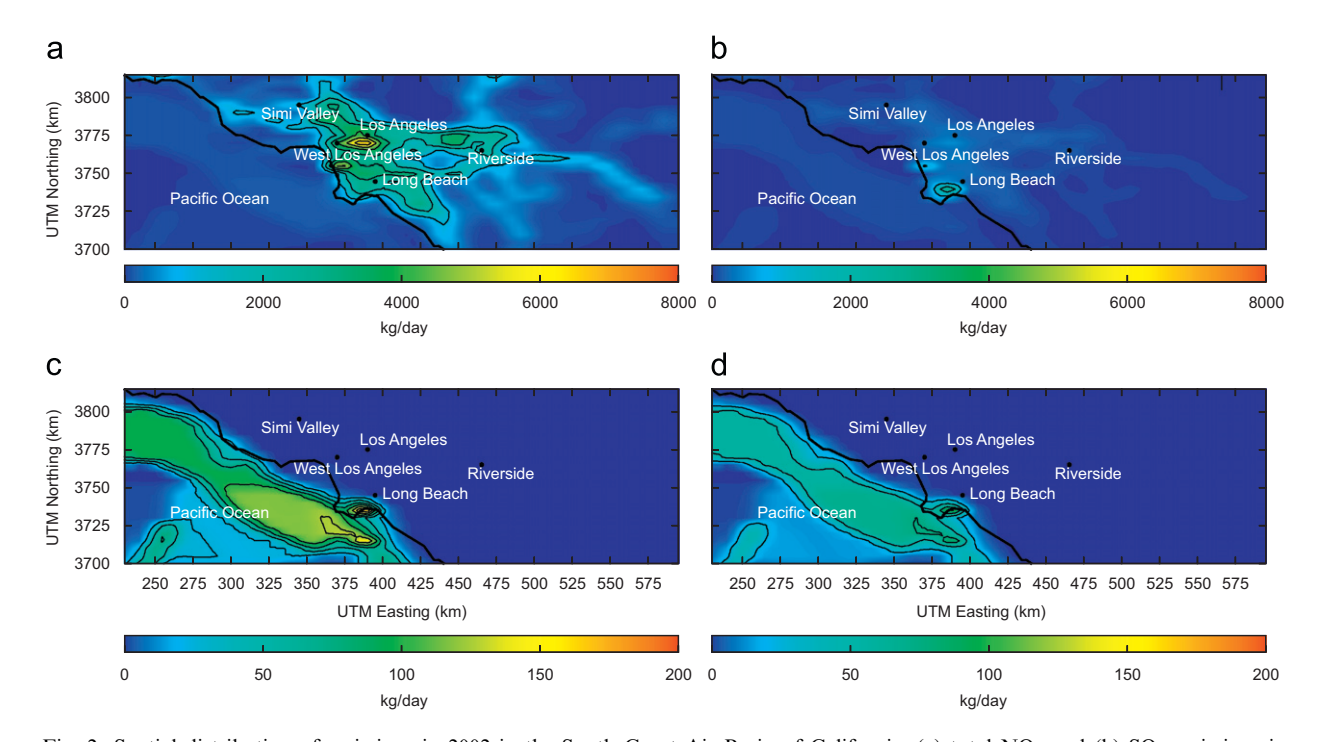


Fig. 2. Spatial distribution of emissions in 2002 in the South Coast Air Basin of California: (a) total  $NO_x$  and (b)  $SO_x$  emissions in  $kg \, day^{-1}$ ; ship emissions of (c)  $NO_x$  and (d)  $SO_x$  in  $kg \, day^{-1}$ .

and from ships only. Emissions of  $NO_x$  and  $SO_x$  are concentrated in urban areas along the coast. Ship emissions occur along the coast of Los Angeles and Ventura counties.

# 3. Impact of ship emissions on air quality

# 3.1. NO2 and SO2 Concentrations

Figs. 3(a) and (b) show 24-h average concentration of  $NO_2$  and  $SO_2$ , respectively, with ship emissions included in the simulation. Only a small fraction of  $NO_2$  is emitted directly. Most of the  $NO_2$  is formed from the photo-oxidation of NO. The distribution of  $NO_2$  is similar to that of emissions of

 $NO_x$  as shown in Fig. 2(a). High concentrations of  $SO_2$  are observed at locations closer to Long Beach where large petroleum refining operations emit high amounts of  $SO_x$ . However,  $SO_2$  concentrations in the areas of Pacific Ocean with ship emissions are comparable to that of inland locations. This is due to relatively high level of  $SO_x$  emissions from ships as shown in Fig. 2.

Figs. 3(c) and (d) show increases in NO<sub>2</sub> and SO<sub>2</sub> concentrations due to ship emissions in 2002. Significant increases are observed in the areas of the Pacific Ocean with direct ship emissions. The increase in these areas is as high as 12 ppb for NO<sub>2</sub> and 4 ppb for SO<sub>2</sub>. Increases in NO<sub>2</sub> are also predicted to occur at locations downwind of ship

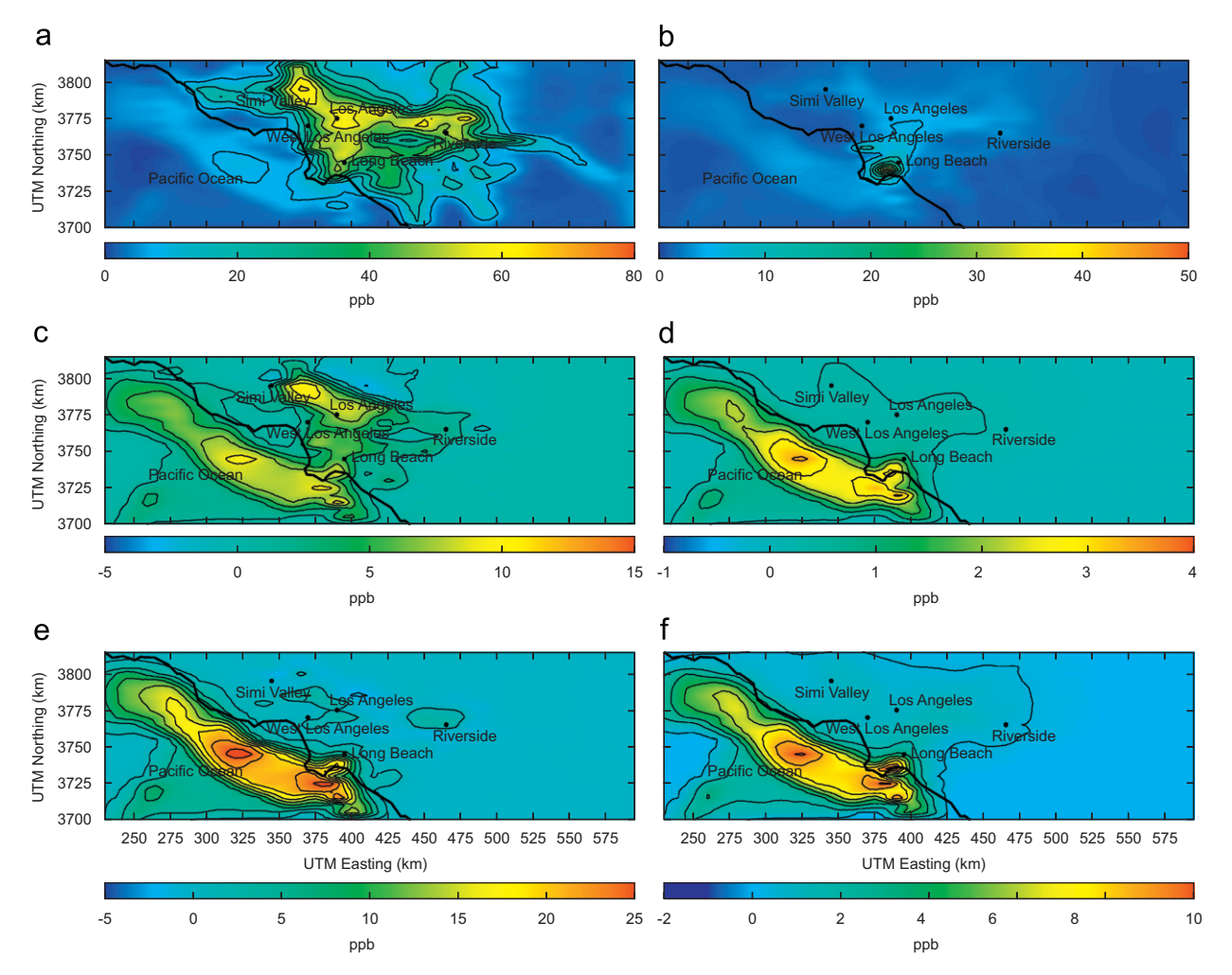


Fig. 3. Impact of ship emissions on  $NO_2$  and  $SO_2$  concentrations in the South Coast Air Basin of California: 24-h average (a)  $NO_2$  concentration and (b)  $SO_2$  concentration with ship emissions for the year 2002. Difference between 24-h average  $NO_2$  concentration for the year (c) 2002 and (e) 2020 for cases with and without ship emissions. Difference between 24-h average  $SO_2$  concentration for the year (d) 2002 and (f) 2020 between cases with and without ship emissions. A positive value indicates an increase in the concentration due to ship emissions. All concentrations are in ppb.

Table 2
Predicted 24-h average concentrations of NO<sub>2</sub> and SO<sub>2</sub> at selected locations in the South Coast Air Basin of California in 2002 and 2020

Location	24-h average	e NO <sub>2</sub> concentr	ration (ppb)	24-h average SO <sub>2</sub> concentration (ppb)			
	Without With Contribution ships ships from ships		Without ships	With ships	Contribution from ships		
2002 case							
Simi Valley	23.3	23.2	-0.1	2.1	2.4	0.3	
West Los Angeles	30.1	33.4	3.3	1.8	2.2	0.4	
Central Los Angeles	51.4	58.8	7.4	4.4	4.7	0.3	
Long Beach	46.2	52.1	5.9	8.2	9.5	1.3	
Riverside	41.4	43.4	2.0	3.9	4.1	0.2	
2020 case							
Simi Valley	9.1	9.7	0.6	2.4	3.4	1.0	
West Los Angeles	11.6	12.6	1.0	2.2	3.1	0.9	
Central Los Angeles	22.2	23.8	1.6	4.5	5.3	0.8	
Long Beach	37.8	46.3	8.5	27.5	32.0	4.5	
Riverside	30.1	33.3	3.2	6.0	6.4	0.4	

emissions, around Los Angeles. The increases at these locations are comparable to areas in the Pacific Ocean with direct NO<sub>x</sub> emissions. In contrast, increases of SO<sub>2</sub> concentrations are less prominent for inland locations and are in the order of 1 ppb. This is due to faster conversion of SO<sub>2</sub> to aerosol sulfate than NO2 to ozone or aerosol nitrate. Table 2 shows increases in 24-h average NO<sub>2</sub> and SO<sub>2</sub> concentrations due to ship emissions at five locations in the domain. NO2 increase ranged from -0.1 to 7.4 ppb at these locations. A negligible decrease is predicted at Simi Valley with relatively low local NO<sub>x</sub> emissions (Fig. 2a), and therefore higher rates of conversion of excess  $NO_x$  from ships to particulate nitrate. NO2 increase at Central Los Angeles is 7.4 ppb followed by Long Beach at 5.9 ppb, both locations are close to the ports and contain high local NO<sub>x</sub> emissions. Increase in SO<sub>2</sub> ranged from 1.2 to 0.2 ppb. The highest impact is predicted to occur at Long Beach, the location closest to port emissions. The lowest impact occurs at Riverside, the farthest location from the port among considered here.

# 3.2. Ambient ozone concentrations

The SoCAB region experiences some of the highest ozone concentrations in the United States, especially during summer months. Ambient ozone concentrations are regulated by the United States federal and California state air quality standards. While the California ozone standard is based on peak 1-h average ozone concentration, federal

ozone standard is based upon 8-h average ozone concentration. The SoCAB is currently designated as a severe non-attainment area towards the compliance with federal 8-h ozone standard. This section presents analysis of increases in predicted maximum 1-h and 8-h average ozone concentrations due to ship emissions.

Figs. 4(a) and (b) show maximum 1-h average and 8-h average ozone concentrations on the final day of the simulation that includes ship emissions in 2002. High ozone concentrations are predicted in eastern part of the domain, downwind of urban coastal areas. In the SoCAB, emissions from coastal urban areas are transported to inland areas, leading to high levels of pollution in the eastern parts of the domain. This trend is in qualitative agreement with previous studies (Griffin et al., 2002; Chock et al., 1999).

Figs. 4(c) and (d) show the difference between maximum 1-h and 8-h average concentrations for cases with ship emissions and without ship emissions. Positive values indicate increase in concentrations due to ship emissions. Significant increases, up to 25 ppb, are observed along the coasts of Los Angeles and Ventura counties, which have relatively clean air without ship emissions. Ship emissions are only local sources of ozone precursors in this part of the domain. Under these conditions when background  $NO_x$  levels are low, the number of ozone molecules produced per nitric oxide molecule is higher than typical urban conditions due to nonlinearity of ozone formation process (Liu et al., 1987). Large increases, up to 29 ppb, are predicted

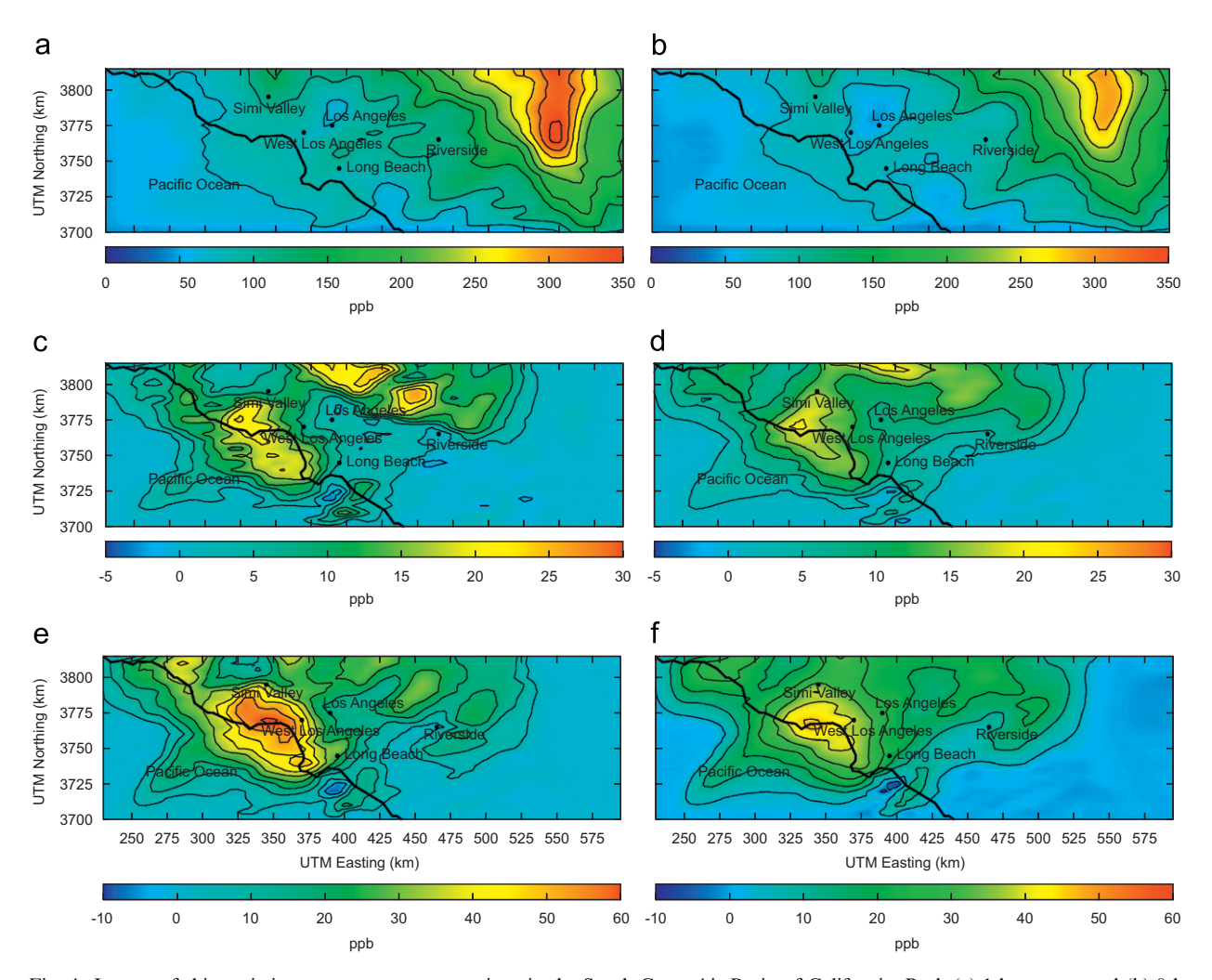


Fig. 4. Impact of ship emissions on ozone concentrations in the South Coast Air Basin of California. Peak (a) 1-h average and (b) 8-h average ozone concentration with ship emissions for the year 2002. Difference between peak 1-h average ozone concentration for years (c) 2002 and (e) 2020 for cases with and without ship emissions. Difference between peak 8-h average ozone concentration for years (d) 2002 and (f) 2020 for cases with and without ship emissions. A positive value indicates an increase in the concentration due to ship emissions. All concentrations are in ppb.

in the region northwest of Los Angeles, downwind of Simi Valley, with already high ozone levels. This is due to daytime sea breeze that moves north of Los Angeles and transports pollutants from coastal regions. Similar trends are observed for increases in maximum 8-h average ozone concentrations as shown in Fig. 4(d). However, in this case the impact of ship emissions has smaller spatial gradients as compared to impact on 1-h ozone concentration. Maximum domain-wide increase in 8-h ozone concentration is 24 ppb and occurs along the coast of Los Angeles.

Increases or decreases in ozone concentrations due to ship emissions are both due to transport of ozone itself from the region of ship traffic, and transport of precursor species ( $NO_x$  and VOCs), which may increase or decrease ozone formation locally. However, the production of ozone is a highly non-linear function of precursor concentrations (Kleinman et al., 1997; Sillman, 1999). Hence the contribution of ship emissions depends upon the intensity of local precursor emissions, especially  $NO_x$  to VOC ratio, and other factors such as temperature. This explains why relatively small increases in ozone from ship emissions are predicted in the Los Angeles area. Region around Los Angeles is  $NO_x$  rich (Griffin et al., 2004) and further increase in  $NO_2$  due to ship emissions leads

to a decrease in ozone concentration. Therefore, the combined effect of transport of ozone and ozone precursors from the region of ship traffic leads to an overall smaller effect from ship emissions in that area as compared to other coastal locations such as West Los Angeles and Long Beach as shown in Fig. 4 (see Table 3).

Table 3 shows increases in maximum 8-h and 1-h average ozone concentrations at Simi Valley, West Los Angeles, Central Los Angeles, Long Beach and Riverside for cases with ship emissions and without ship emissions. For these locations, increases in 8-h concentrations ranged from 4.3 to 16.4 ppb. The range of impact on 1-h ozone concentrations is -0.5to 8.1 ppb. For both metrics, the minimum impact is predicted at Riverside—the farthest location from the coast among considered here. A small decrease in the maximum 1-h ozone concentration (0.5 ppb) at Riverside is predicted when ship emissions are included. Riverside is significantly impacted by atmospheric transport of ozone, NOx and VOCs from upwind locations. The introduction of NO<sub>x</sub> from ship emissions in upwind areas results in the reduction of concentration of VOCs at Riverside at the hour of occurrence of peak ozone concentration. This leads to a small decrease in peak ozone at Riverside. However, 8-h average ozone concentration increases at Riverside by 4.3 ppb since ship emissions leads to ozone increase at other times during the day.

Lawrence and Crutzen (1999) reported the increase in summertime average ozone concentration by 10% in the Southern California region using

a global model and 1993 emission inventories on a coarse grid. When 24-h ozone averages are calculated using results from this study over aggregated cells around the ports with area similar to those in global models  $(1^{\circ} \times 1^{\circ})$ , increase in ozone is 9%. Therefore, the impacts from this regional-scale modeling study are in the same range as coarser scale studies. However, this study shows how individual locations are affected to a varying extent, given much smaller spatial scales and the use of more detailed physical and chemical mechanisms. For instance, the corresponding percentage increase in 24-h average ozone concentrations due to ship emissions from this work is 35% at Simi Valley, 32% at West Los Angeles, 26% at Central Los Angeles, 13% for Long Beach and 1% for Riverside locations.

## 3.3. Ambient PM concentrations

Ambient PM is linked to adverse health effects and hence is designated as a criteria pollutant by the United States Environmental Protection Agency. Southern California region exhibits some of the highest levels of ambient PM and experiences large number of days with ambient PM concentrations exceeding the state and federal air quality standards (CARB, 2007). Besides direct emission of particles from combustion and other sources, a significant fraction of this PM is formed through secondary processes from gas-phase emissions. As previous modeling and field studies showed, particulate

Table 3
Predicted ozone concentrations at selected locations in the South Coast Air Basin of California in 2002 and 2020

Location	Peak 1-h oz	one concentrati	on (ppb)	Peak 8-h ozone concentration (ppb)			
	Without ships			Without ships	With ships	Contribution from ships	
2002 case							
Simi Valley	116.0	124.1	8.1	87.8	104.2	16.4	
West Los Angeles	60.6	68.8	8.2	45.1	58.2	13.1	
Central Los Angeles	56.0	60.5	4.5	37.1	45.0	7.9	
Long Beach	86.1	92.4	6.3	69.8	76.2	6.4	
Riverside	110.5	110.0	-0.5	82.2	86.5	4.3	
2020 case							
Simi Valley	86.1	123.4	37.3	67.4	107.2	39.8	
West Los Angeles	57.9	112.0	54.1	52.4	89.9	37.5	
Central Los Angeles	104.0	121.1	17.1	79.8	107.1	27.3	
Long Beach	82.8	117.4	34.6	70.6	96.8	26.2	
Riverside	100.1	101.9	1.8	80.0	86.4	6.4	

nitrates and sulfates formed from  $NO_x$  and  $SO_x$  emissions are major components of PM in the SoCAB (Sawant et al., 2004; Kim et al., 2000). In this section, contribution of ship emissions to ambient PM is quantified by analyzing model-predicted PM concentrations for cases with and without ship emissions.

Figs. 5(a) and (b) show 24-h average concentrations of  $PM_{2.5}$  nitrate and sulfate on the final day of simulation that includes ship emissions. The peak  $PM_{2.5}$  nitrate concentration is approximately  $61 \, \mu g \, m^{-3}$  and occurs in the inland portion of the domain, northeast of Riverside. This regional distribution is in qualitative agreement with pre-

vious modeling and measurement studies (Ying and Kleeman, 2006; Sawant et al., 2004; Kim et al., 2000). Although NO<sub>x</sub> emissions are mainly concentrated in the coastal areas, formation of particulate nitrate as ammonium nitrate (NH<sub>4</sub>NO<sub>3</sub>) is limited by the availability of gas-phase ammonia (Nguyen and Dabdub, 2002a). Presence of ammonia emissions from dairy operations in the Riverside area and transport of NO<sub>x</sub> to inland areas leads to this regional distribution. The peak PM<sub>2.5</sub> sulfate concentration is predicted to occur in the Long Beach area, a coastal location. This is due to intense direct sulfate and SO<sub>x</sub> emissions from large petroleum refinery operations in the area (Ying and Kleeman,

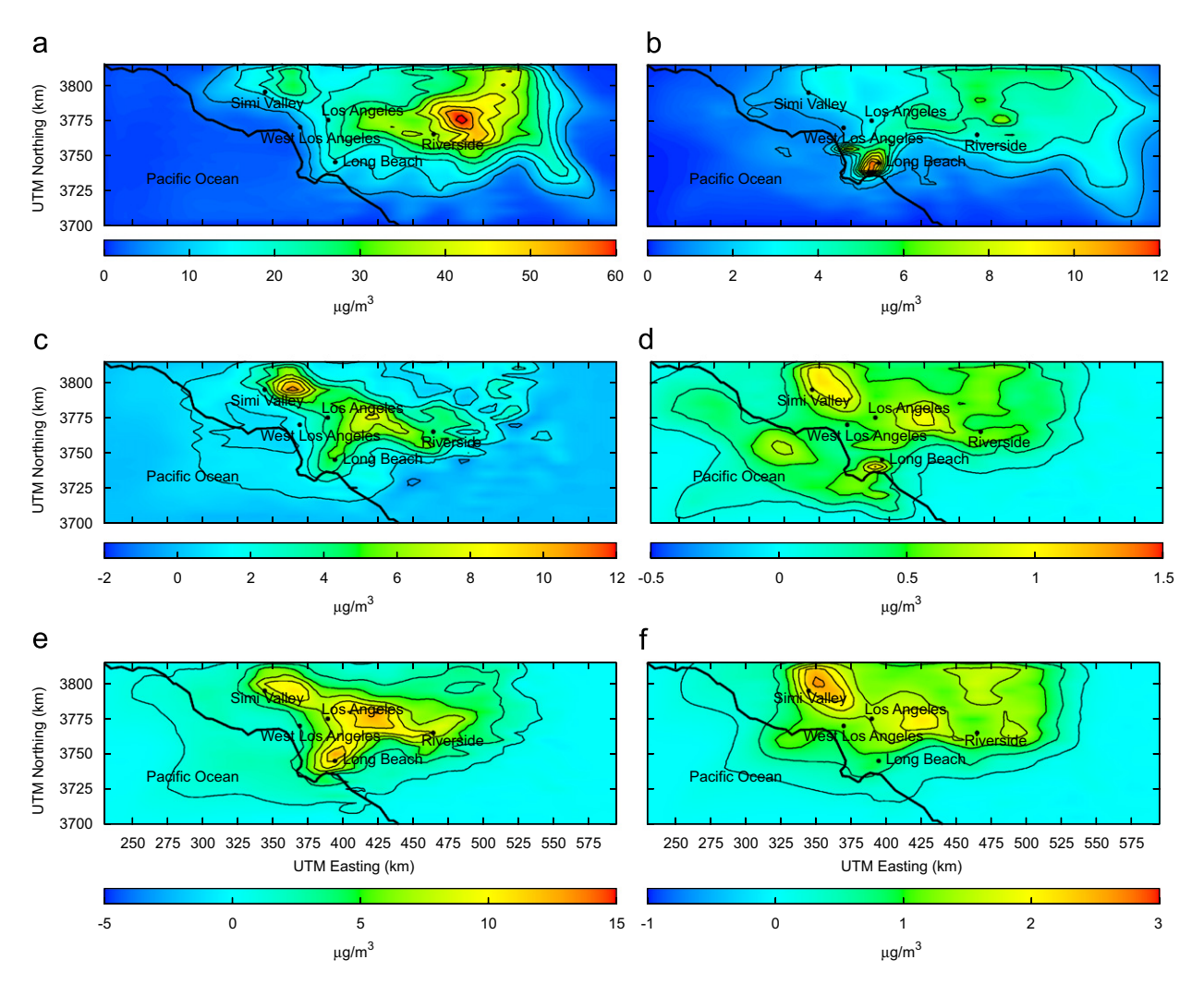


Fig. 5. Impact of ship emissions on PM concentrations in the South Coast Air Basin of California: 24-h average concentration of particulate (a) nitrate and (b) sulfate with ship emissions for the year 2002. Difference between 24-h average concentration of particulate nitrate for years (c) 2002 and (e) 2020 for cases with and without ship emissions. Difference between 24-h average concentration of particulate sulfate for years (d) 2002 and (f) 2020 for cases with and without ship emissions. A positive value indicates an increase in the concentration due to ship emissions. All concentrations are in  $\mu$ g m<sup>-3</sup>.

2006). For inland locations, PM<sub>2.5</sub> sulfate is more uniformly distributed than PM<sub>2.5</sub> nitrate.

Figs. 5(c) and (d) show 24-h average concentration difference between cases with and without ship emissions for  $PM_{2.5}$  nitrate and sulfate, respectively. The maximum model-predicted increase for  $PM_{2.5}$  nitrate is  $12.8\,\mu g\,m^{-3}$  and that for  $PM_{2.5}$  sulfates is  $1.7\,\mu g\,m^{-3}$ . Maximum increases for both species are predicted to occur in northern part of the domain, east of Simi Valley. In addition, a region of significant increases for both particulate nitrate and sulfate is predicted to occur between Los Angeles and Riverside.

Table 4 shows increase in sulfate, nitrate and total PM<sub>2.5</sub> concentrations at five locations in the basin: Simi Valley, West Los Angeles, Central Los Angeles, Long Beach and Riverside. The increases range from 1.7 to  $6.7 \,\mu\mathrm{g}\,\mathrm{m}^{-3}$  for nitrate and 0.4 to 1.0 µg m<sup>-3</sup> for sulfate concentrations. Riverside, an inland location about 100 km from the coast, is predicted to experience an increase in PM2.5 concentration by  $4.3 \,\mu\mathrm{g}\,\mathrm{m}^{-3}$  due to particulate nitrates and sulfates together. Capaldo et al. (1999) showed an increase in sulfate concentrations by 5–20% due to ships in areas closer to the coast in Southern California using the GFDL global model. The corresponding increase from this work in sulfate concentrations is 5.3% at Long Beach, and 30% at West Los Angeles—two locations that are closer to the coast.

PM<sub>2.5</sub> increases at the five locations discussed previously ranged from 9.2 to 4.5 μg m<sup>-3</sup> (Table 4). Contribution from sulfates and nitrates together accounts for a major fraction of increase in total PM<sub>2.5</sub>. The remaining increase in total PM<sub>2.5</sub> is attributed to uptake of additional ammonia and increase in secondary organic aerosol (SOA) formation. Although VOC emissions, which are precursor species of SOA, are small from ships, the enhanced oxidation capacity of the atmosphere due to ozone increase (Section 3.2) leads to enhanced production of SOA (Vutukuru et al., 2006) thus contributing to an increase in total PM<sub>2.5</sub>.

Direct PM emissions from ships contain a significant amount of sulfate particles due to high sulfur content in marine fuels (Entec, 2002). As discussed in Section 2.2, 45% of total directly emitted PM from ships is in the form of sulfates. However, direct PM mostly affects the region of ship emissions as these particles are deposited rapidly on to the surface. Furthermore, nitrates contribute significantly to total PM<sub>2.5</sub> impacts although particulate nitrates in the form of direct PM emissions are negligible (0.01% of direct PM is assumed to be nitrates using the CARB speciation profile). Therefore, most of the contribution from ships to PM at inland locations comes as secondary PM from gas-phase emissions. The formation of secondary PM is heavily influenced by the OH radical concentration. Reaction of OH with SO<sub>2</sub>

Table 4
Predicted 24-h average concentrations of particulate nitrate, sulfate and total PM<sub>2.5</sub> at selected locations in the South Coast Air Basin of California in 2002 and 2020

Location	24-h average nitrate concentration $(\mu g  m^{-3})$			24-h average sulfate concentration $(\mu g  m^{-3})$			24-h average total $PM_{2.5}$ concentration $(\mu g  m^{-3})$		
	Without ships	With ships	Contribution from ships	Without ships	With ships	Contribution from ships	Without ships	With ships	Contribution from ships
2002 case									
Simi Valley	9.1	10.8	1.7	1.4	2.4	1.0	32.2	36.7	4.5
West L.A.a	2.8	4.8	2.0	0.8	1.3	0.4	18.6	22.9	4.3
Central L.A.a	14.5	18.2	3.7	2.5	2.9	0.1	66.6	71.8	5.2
Long Beach	14.4	21.1	6.7	10.6	11.3	0.6	84.0	93.0	9.0
Riverside	31.4	35.2	3.8	3.5	4.0	0.5	91.3	100.5	9.2
2020 case									
Simi Valley	3.2	10.4	7.2	1.5	3.9	2.4	24.8	40.5	15.7
West L.A.a	1.5	4.4	2.9	1.1	2.2	1.1	15.8	23.1	7.3
Central L.A.a	8.7	15.7	7.0	2.4	3.8	1.4	58.2	71.8	13.5
Long Beach	15.5	31.1	15.6	16.8	18.0	1.2	93.2	119.5	26.2
Riverside	17.0	24.2	7.2	4.5	5.6	1.1	83.1	94.0	10.9

<sup>&</sup>lt;sup>a</sup>L.A., Los Angeles.

and  $NO_2$  forms gas-phase  $H_2SO_4$  and  $HNO_3$ , respectively. Gas-phase  $HNO_3$  forms  $NH_4NO_3$  in the particulate phase through reaction with  $NH_3$ , and  $H_2SO_4$  enters particulate phase through nucleation or condensation on existing aerosol particles. Since ozone is a dominant source of OH radicals in the urban atmosphere, high ozone concentrations in the basin lead to efficient conversion of  $NO_x$  and  $SO_x$  from ships to particulate nitrate and sulfates (Meng et al., 1997; Nguyen and Dabdub, 2002a).

# 4. Future year impacts

Ship emissions are predicted to increase significantly due to increase in ship traffic (Eyring et al., 2005). Indirect indicators of ship activity such as goods movement, fraction of international trade as a proportion of US gross domestic product are estimated to grow over 6% per year (Corbett et al., 2007). On the other hand, land-based emissions are projected to decrease due to environmental regulation. Therefore, ship emissions will form a significant portion of regional emission inventories. In this section, the impact of ship emissions for the year 2020 on ozone and PM is quantified using the summer air quality episode described in previous sections.

Corbett et al. (2007) forecasted ship emissions 2020 by considering potential changes in emission factors, engine sizes, vessel numbers and fuel quality. Using these forecasts, ship emissions for a summer day in 2020 are developed as described for the baseline year. Land-based emissions are developed from the 2010 baseline emissions used in the AQMP 2003 plan developed by the South Coast Air Quality Management District. These emissions are scaled to 2020 levels using county-wide factors from emission projections of CARB. Table 1 summarizes estimated total domain-wide and ship emissions for the year 2020. Estimated daily emissions of  $NO_x$ and  $SO_x$  from ships are 97.9 and 59.1 ton, respectively.  $SO_x$  and  $NO_x$  emissions from ships contribute almost 40% and 25% of total emissions in the basin, respectively, a dramatic increase from 2002 levels. This is due to both increase in NO<sub>x</sub> emissions from ships and anticipated decrease in NO<sub>x</sub> emissions from land-based sources. Contribution of VOCs is expected to remain less than 2% and that of PM less than 0.5% of domain-wide emissions.

Figs. 3(e) and (f) show predicted increase in 24-h average concentrations of NO<sub>2</sub> and SO<sub>2</sub> in the

SoCAB for 2020. High impacts for both species are predicted in the region of ship emissions. These increases are as high as 24 ppb for NO<sub>2</sub> and 9 ppb for SO<sub>2</sub>, which are almost twice the values predicted for 2002. Table 2 shows impact on NO<sub>2</sub> and SO<sub>2</sub> at five sites in the basin. Long Beach is predicted to experience the maximum increase of 8.5 and 4.5 ppb in NO2 and SO2 concentration, respectively. Predicted NO<sub>2</sub> increases are smaller than those for 2002 at some locations. This is due to major reductions in local NO<sub>x</sub> emissions leading to more efficient conversion of excess NO<sub>x</sub> emissions from ships to PM nitrate (Fig. 5e). However, SO<sub>2</sub> concentrations increase consistently at all locations and are more than two to three times higher than those predicted for 2002.

Figs. 4(e) and (f) show predicted increase in 1-h and 8-h ozone concentrations in the SoCAB for 2020. Peak impacts of 59 and 45 ppb on 1-h and 8-h ozone concentration, respectively, are predicted to occur along the coast of Los Angeles and Ventura Counties. Ship emissions are the primary source of emissions at these locations and hence high impacts are predicted. Some inland sites experience an increase in maximum 1-h and 8-h concentration as high as 30 ppb due to atmospheric transport of precursor species and ozone itself. Table 3 shows peak 1-h and 8-h ozone concentrations at five locations in the basin. Ships contribute significantly to ozone at all these locations, especially West Los Angeles and Long Beach.

Figs. 5(e) and (f) shows difference between 24-h average concentrations for particulate nitrate and sulfates between cases with and without ship emissions for the year 2020. Maximum impacts are observed at sites downwind of Simi Valley, Los Angeles and Long Beach. The highest impact is predicted to occur downwind of Los Angeles and is about  $14 \,\mu \text{g m}^{-3}$ . Although NO<sub>x</sub> emissions from ships increase significantly from 2002 levels, there is no corresponding increase in particulate nitrate concentrations since nitrate formation is limited by the availability of gas-phase NH<sub>3</sub>. However, increase of SO<sub>x</sub> from ship emissions leads to an increase in particulate sulfates. The maximum increase in particulate sulfates is about  $2.5 \,\mu \mathrm{g \, m}^{-3}$ and is predicted to occur downwind of Simi Valley. In contrast to impacts predicted for 2002, particulate sulfate from ships is observed in eastern portions of the domain in the excess of  $1 \mu g \, m^{-3}$ . Table 4 shows 24-h average concentrations of particulate nitrate and sulfate, and total PM<sub>2.5</sub> for

five locations in the basin for 2020. Particulate nitrate and sulfate together constitute a major fraction of total increase in  $PM_{2.5}$  at all of these locations. The remainder of total  $PM_{2.5}$  increase is mostly from ammonia uptake and SOA formation. West Los Angeles and Long Beach experience additional contribution from direct PM emissions leading to a further increase in total  $PM_{2.5}$ . The maximum increase of  $26.2\,\mu g\,m^{-3}$  in total  $PM_{2.5}$  is predicted at Long Beach. A significant increase in particulate nitrate is predicted at Riverside  $(7.2\,\mu g\,m^{-3})$ , an inland location, underlining the importance of atmospheric transport of ship emissions and secondary PM formation.

## 5. Conclusion

This study illustrates the use of regional air quality models to assess the impact of ships at locations close to ports and shipping routes. A comprehensive gas-phase chemical mechanism, such as CACM, enables the prediction of impacts on peak 1-h and 8-h ozone concentrations that are important from regulatory perspective. Furthermore, a coupled aerosol mode provides an accurate treatment of secondary aerosol formation leading to quantifiable impacts on 24-h average PM impacts. Results show that individual locations are impacted at different levels depending on local emissions. Results from this study, in combination with population data, are useful in assessing health impacts of ship emissions.

This study quantifies the effects of ship emissions on air quality in Southern California using the UCI-CIT model. Presence of two major ports in the region, coupled with unique topographical and meteorological features leads to increases in ozone, particulate sulfates and nitrates in the region. For the year 2002, ships emitted 38.4 and 22.8 ton day<sup>-1</sup> of  $NO_x$  and  $SO_x$  emissions, respectively, in the model domain. Analysis of model runs with and without ship emissions show that ship emissions contribute significantly to ozone and PM concentrations at many coastal locations. Maximum increase of 29 and 24 ppb in peak 1-h and 8-h average ozone concentrations, respectively, is predicted due to NO<sub>x</sub> from ships. Similarly, 24-h average particulate nitrate and sulfate concentrations increase up to 12 and 1.25 µg m<sup>-3</sup> due to ship emissions. Inland locations also experience increase in ozone and PM concentrations, although at smaller magnitudes in comparison with coastal

locations. As land-based emissions decline in future years due to emission regulations, ship emissions become increasingly important. Model runs using emission estimates for 2020 show that ships could become a major source of air pollution in the region.

# Acknowledgments

This work is partly funded by California Air Resources Board (CARB) contract 04-752. The views presented here are solely those of authors. We thank Dr. Ajith Kaduwela and Dr. Dongmin Luo of CARB for helpful discussions. We thank Tony Soeller of Network and Academic Computing Services at University of California, Irvine, for his help in preparing ship emission input files using GIS tools.

# References

- BST Associates, 2007. Trade impacts study. Prepared for Port of Los Angeles, Port of Long Beach and Almeda Corridor Transportation Authority <a href="http://www.portoflosangeles.org/DOC/REPORT">http://www.portoflosangeles.org/DOC/REPORT</a> ACTA Trade Impact Study.pdf>.
- California Air Resources Board, 2007. Historical air quality data. Available at: <a href="http://www.arb.ca.gov/aqd/aqdpage.htm">http://www.arb.ca.gov/aqd/aqdpage.htm</a>.
- Capaldo, K., Corbett, J.J., Kasibhatla, P., Fischbeck, P., Pandis, S.N., 1999. Effects of ship emissions on sulphur cycling and radiative climate forcing over the ocean. Nature 400, 743–746.
- Carreras-Sospedra, M., Griffin, R.J., Dabdub, D., 2005. Calculation of incremental secondary organic aerosol reactivity. Environmental Science and Technology 38, 1724–1730.
- Carreras-Sospedra, M., Rodriguez, M., Brouwer, J., 2006. Air quality modeling in the South Coast Air Basin of California: what do the numbers really mean? Journal of Air and Waste Management Association 56, 1184–1995.
- Chock, D.P., Chang, T.Y., Winkler, S.L., Nance, B.I., 1999. The impact of an 8 h ozone air quality standard on ROG and NO<sub>x</sub> controls in Southern California. Atmospheric Environment 33 (16), 2471–2485.
- Corbett, J.J., Fischbeck, P.S., 1997. Emissions from ships. Science 278, 823–824.
- Corbett, J.J., Koehler, H.W., 2003. Updated emissions from ocean shipping. Journal of Geophysical Research 108 (D20), 4650.
- Corbett, J.J., Fischbeck, P.S., Pandis, S.N., 1999. Global nitrogen and sulfur emissions inventories for oceangoing ships. Journal of Geophysical Research 104 (D3), 3457–3470.
- Corbett, J.J., Firestone, J., Wang, C., 2007. Estimation, validation and forecasts of regional commercial maritime vessel inventories. Prepared for California Air Resources Board. Available at: <a href="http://www.arb.ca.gov/research/seca/jcfinal.pdf">http://www.arb.ca.gov/research/seca/jcfinal.pdf</a>.
- Derwent, R.G., Stevenson, D.S., Doherty, R.M., Collins, W.J., Sanderson, M.G., Johnson, C.E., Cofala, J., Mechler, R., Amann, M., Dentener, F.J., 2005. The contribution from

- shipping emissions to air quality and acid deposition in Europe. AMBIO 34 (1), 54-59.
- Dore, A.J., Vieno, M., Tang, Y.S., Dragosits, U., Dosio, A., Weston, K.J., Sutton, M.A., 2007. Modelling the atmospheric transport and deposition of sulphur and nitrogen over the United Kingdom and assessment of the influence of SO<sub>2</sub> emissions from international shipping. Atmospheric Environment 41 (11), 2355–2367.
- Endresen, O., Sorgard, E., Sundet, J.K., Dalsoren, S.B., Isaksen, I.S.A., Berglen, T.F., Gravir, G., 2003. Emission from international sea transportation and environmental impact. Journal of Geophysical Research 108 (D17), 4560.
- Entec UK Limited, 2002. European Commission: quantification of emissions from ships associated with ship movements between ports in the European Community. Final Report, London, UK.
- Eyring, V., Kohler, H.W., Lauer, A., Lemper, B., 2005. Emissions from international shipping: 2. Impact of future technologies on scenarios until 2050. Journal of Geophysical Research 110 (D17), D17306.
- Griffin, R.J., Dabdub, D., Seinfeld, J.H., 2002. Secondary organic aerosol: 1. Atmospheric chemical mechanism for production of molecular constituents. Journal of Geophysical Research 107 (D17), 4332.
- Griffin, R.J., Revelle, M.K., Dabdub, D., 2004. Modeling the oxidative capacity of the atmosphere of the South Coast Air Basin of California. 1. Ozone formation metrics. Environmental Science and Technology 38, 746–752.
- Harley, R.A., Cass, G.R., 1994. Modeling the concentrations of gas-phase toxic organic air pollutants: direct emissions and atmospheric formation. Environmental Science and Technology 28, 88–98.
- International Maritime Organization, 2000. Report on the outcome of the IMO study on greenhouse gas emissions from ships. MEPC 45/8. International Maritime Organization, London.
- Kim, B.M., Teffera, S., Zeldin, M.D., 2000. Characterization of PM<sub>2.5</sub> and PM<sub>10</sub> in the South Coast Air Basin of Southern California: part 1—spatial variations. Journal of the Air and Waste Management Association 50 (12), 2034–2044.
- Kleinman, L.I., Daum, P.H., Lee, J.H., Lee, Y., Nunnermacker, L.J., Springston, S.R., Newman, L., 1997. Dependence of ozone production on NO and hydrocarbons in the troposphere. Geophysical Letters 24 (18), 2299–2302.
- Knipping, E.M., Dabdub, D., 2003. Impact of chlorine emissions from sea-salt aerosol on coastal urban ozone. Environmental Science and Technology 37, 275–284.
- Lawrence, M.G., Crutzen, P.J., 1999. Influence of  $NO_x$  emissions from ships on tropospheric photochemistry and climate. Nature 402 (6758), 167–170.
- Liu, S.C., Trainer, M., Fehsenfeld, F.C., Parrish, D.D., Williams, E.J., Fahey, D.W., Hubler, G., Murphy, P.C., 1987. Ozone production in the rural troposphere and the implications for regional and global ozone distributions. Journal of Geophysical Research 92, 4191–4207.
- Lu, G., Brook, J.R., Alfarra, M.R., Anlauf, K., Leaitch, W.R., Sharma, S., Wang, D., Worsnop, D.R., Phinney, L., 2006. Identification and characterization of inland ship plumes

- over Vancouver, BC. Atmospheric Environment 40 (15), 2767-2782.
- McRae, G.J., Seinfeld, J.H., 1982. Development of a secondgeneration mathematical model for urban air pollution. 1. Model formulation. Atmospheric Environment 16, 679–696.
- Meng, Z., Dabdub, D., Seinfeld, J.H., 1997. Chemical coupling between atmospheric ozone and particulate matter. Science 277 (5322), 116–119.
- Meng, Z., Dabdub, D., Seinfeld, J.H., 1998. Size-resolved and chemically resolved model of atmospheric aerosol dynamics. Journal of Geophysical Research 103, 3419–3435.
- Nguyen, K., Dabdub, D., 2001. Two level time marching scheme using splines for solving the advection equation. Atmospheric Environment 35, 1627–1637.
- Nguyen, K., Dabdub, D., 2002a. NO<sub>x</sub> and VOC control and its effect on the formation of aerosols. Aerosol Science and Technology 36, 560–572.
- Nguyen, K., Dabdub, D., 2002b. Semi-Lagrangian flux scheme for the solution of the aerosol condensation/evaporation equation. Aerosol Science and Technology 36, 407–418.
- Richter, A., Eyring, V., Burrows, J.P., Bovensmann, H., Lauer, A., Sierk, B., Crutzen, P., 2004. Satellite measurements of NO<sub>2</sub> from international shipping emissions. Geophysical Research Letters 31, L23110.
- Rodriguez, M., Dabdub, D., 2003. Monte Carlo uncertainty and sensitivity analysis of the CACM chemical mechanism. Journal of Geophysical Research 108 (D15), 4443.
- Rodriguez, M., Carreras-Sospedra, M., Medrano, M., Brouwer, J., Samuelsen, G.S., Dabdub, D., 2006. Air quality impacts of distributed power generation in the South Coast Air Basin of California 1: scenario development and modeling analysis. Atmospheric Environment 40, 5505–5521.
- Sawant, A.A., Na, K., Zhu, X.N., Cocker, D.R., 2004. Chemical characterization of outdoor PM<sub>2.5</sub> and gas-phase compounds in Mira Loma, California. Atmospheric Environment 38 (33), 5517–5528.
- Sillman, S., 1999. The relation between ozone, NO<sub>x</sub> and hydrocarbons in urban and polluted rural environments. Atmospheric Environment 33 (12), 1821–1845.
- Streets, D.G., Guttikunda, S.K., Carmichael, G.R., 2000. The growing contribution of sulfur emissions from ships in Asian Waters, 1998–2005. Atmospheric Environment 34, 4425–4439.
- Vutukuru, S., Griffin, R.J., Dabdub, D., 2006. Simulation and analysis of secondary organic aerosol dynamics in the South Coast Air Basin of California. Journal of Geophysical Research 111 (D10S12), 1.
- Wang, C., Corbett, J.J., Firestone, J., 2007. Modeling energy use and emissions from North American shipping: application of the ship traffic, energy, and environment model. Environmental Science and Technology 41 (9), 3226–3232.
- Ying, Q., Kleeman, M., 2006. Source contributions to the regional distribution of secondary particulate matter in California. Atmospheric Environment 40, 736–752.
- Zeldin, M.D., Bregman, L.D., Horie, Y.A., 1990. Meteorological and air quality assessment of the representativeness of the 1987 SCAQS intensive days. Final report to the South Coast Air Quality Management District, Diamond Bar, CA.